Proceedings World Geothermal Congress 2015
Melbourne, Australia, 19-25 April 2015

Resistivity Image of the San Andreas Fault System around the Cerro Prieto Geothermal Area (México)

Pérez-Flores, M.A., Herrera-Barrientos, F., Gómez-Trevino, E. Salomé-Charre, A, Romo-Jones, J.M., Gallardo-Delgado, A., Brassea-Ochoa, J., Esparza, F.J. and Flores-Luna, C.

División de Ciencias de la Tierra, Carretera Ensenada-Tijuana #3918, Zona Playitas, Ensenada, Baja California, México.

mperez@cicese.mx, fherrera@cicese.mx, egomez@cicese.mx, jromo@cicese.mx, lgallard@cicese.mx, jbrassea@cicese.mx, fesparz@cicese.mx, cflores@cicese.ms.

Keywords: resistivity, image, Cerro Prieto, pull-apart basin.

ABSTRACT

In 1978 and 1979 the Lawrence Berkeley National Laboratory (LBNL) in collaboration with Comisión Federal de Electricidad (CFE) took 411 long-range Schlumberger soundings along 20 lines distributed around the Cerro Prieto Geothermal area. This information was processed and interpreted with the technology of those times. Presently, we reused that information and interpreted it using 3D constrained inversion. The 3D resistivity model shows a conductive thin overburden over a more resistive layer with varying thickness (~600 m) associated with Colorado River alluvial deposits. Below a depth of 1000 m, there are alignments clearly related to the Cerro Prieto and Imperial faults (local names for the San Andreas fault system), which are the principal faults of the Mexicali Rift Valley. Both faults appear as straight narrow conductive zones offset laterally from each other by the central rift valley, which has a more complex resistivity structure.

1. INTRODUCTION

Presently, the San Andreas fault forms the contact between the North American and Pacific plates. In the past, there was subduction of the Farallon plate under the North American plate. The Farallon plate was consumed and the subduction movement stopped (Aragon-Arreola and Martin-Barajas, 2007). Then, 12 Ma ago the separation of the Baja California peninsula began (proto-gulf). This movement continues until now and the past is recorded on the sea floor in the form of spreading centers connected by transform faults, forming a submarine system of pull-apart basins as seen in Figure 1. The Baja California peninsula separation began at the southward end and the separation has been continued until the Mexicali Valley. This area is interesting, because it is an on-land continuation of the spreading center to the north. The Cerro Prieto area or the Mexicali valley is over one portion of this spreading center. Because of the tectonics, this area has been submerged and subsequently uplifted, showing a considerable thickness of marine and deltaic sediments in the form of claystone, mudstone and sandstone sequences as can be shown at the western side of the El Mayor Sierra, SW of the Mexicali Valley (Dorsey and Martin-Barajas, 1999). These sediments are very salty and therefore are electrically conductive. The Colorado River has also contributed with fluvial sediments and the Mexicali Valley has been irrigated from the NE, with drainage towards SW. Thanks to this on-land spreading center the Cerro Prieto Geothermal field exists.

Figure 1: The San Andreas fault marks the boundary between the North American and Pacific plates. It caused the separation of the Baja California peninsula. A system of spreading centers connected by transform faults northward is located on the sea floor. Mexicali valley is outlined by the red box.

2. METHOD

Berkeley Lab in 1978 took more than 400 long-range Schlumberger soundings (SEV's) around the Cerro Prieto Geothermal field or the Mexicali Valley (Wilt et al., 1978). They used the direct current geophysical method (zero frequency). They injected a very large amount of current in the ground and they used large and special electric generators. It was a costly and difficult field project considering the extreme hot temperatures at the area (50°C). It took more than a year to complete the field work. The largest source-received distance used was 5 km. With such a distance, it is possible to penetrate close to 2 km depth, depending on the ground resistivity. The more conductive, the less penetration and vice versa.

The SEV's centers were distributed on SW-NE lines as shown in Figure 2. Every point represents an SEV center. However, many measurements were taken with the same center, varying the source-receiver distance until 5 m. The measurements spread around the center in the same SW-NE direction. That was very helpful in order to try 2D modeling or 2D inversion. In those days the interpretation was done by trial and error, fitting the data with the model response. The resulting model was blocky but with very good resemblance with the present 2D inversion methods (Wilt et al., 1979). In Charre (2000), we presented the 2D models for every line using least squares inversion and compared them with the trial and error models. The problem with 2D inversion is that we assume that every 2D model is independent. That could be true in lines with large separation between them, but not in closer lines. By assuming 2D independent models, we fit the 3D effects as high spatial frequency 2D bodies that do not exist. It is better to consider those effects and not evaluate them as overburden effects. In this research, we used the 3D constrained inversion method developed by Perez-Flores et al. (2001).

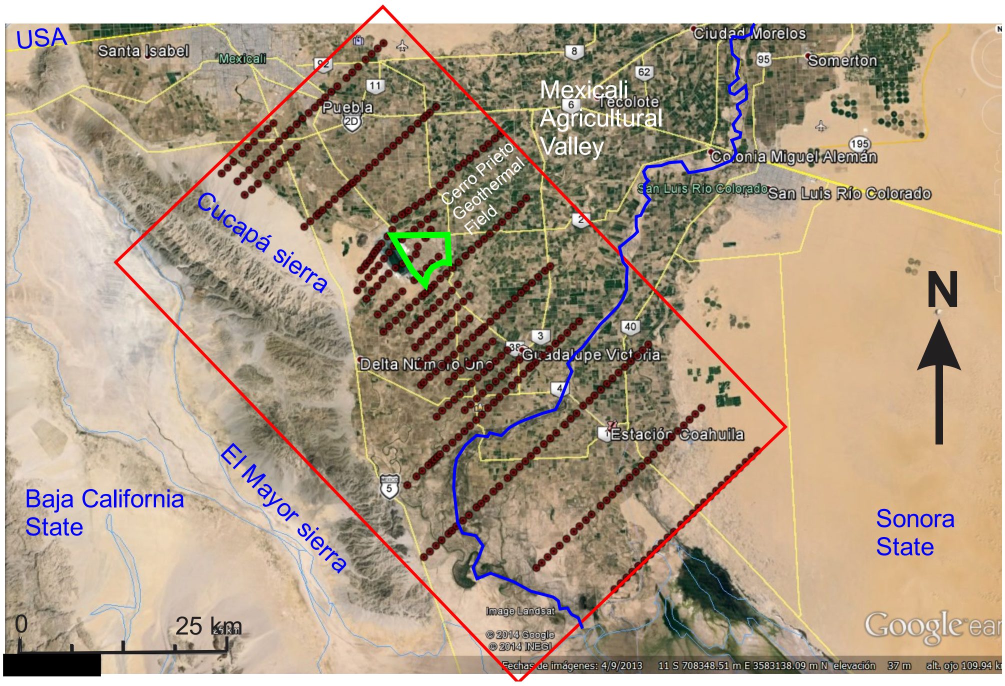

Figure 2: The Mexicali Valley with the USA border northward. Brown dots show the SEV's center locations. The red box is the area considered for the 3D inversion. Sierras are present westward of the inversion area. The green polygon shows the present geothermal area. The blue line represents the Colorado River (flowing southward).

We took a rectangular piece of the Mexicali valley as shown in Figure 2 and discretized it using several layers of 3D prisms. This rectangular area was rotated for easier calculations. The 3D prism grid has a constant 1 km width in the x-direction and 5 km in the y-direction. Along the z-direction, several 3D prisms are assumed. Every layer has a constant z-thickness, but the thickness varies from layer to layer. We assumed a logarithmic increase in the z-thickness width with depth. We minimized the quadratic difference of the data and the model response. The inversion process estimated the resistivity for every prism. We also minimized the horizontal and vertical derivatives of the spatial resistivity. This way, we avoid unnecessary high-frequency features in the 3D resistivity model. We used the Gill et al. (1986) code for quadratic programming. Therefore, we can also put constraints on the resistivities to be computed.

3. RESULTS

Figure 3 shows the 3D resistivity model obtained after the constrained inversion. The dots show the SEV locations. In Figure 3a are shown the horizontal dimensions for every prism. It was discretized finer in the x-direction and broader in the y-direction because of the data distribution. The misfit was 17%. It was chosen as a smooth model (resistivity derivatives minimization) because data are not very well distributed. We have no data over the sierra area, so we decided to constraint those prisms to being very resistive.

Figure 3a shows a very shallow slice and reflects the conductor overburden all along the Mexicali valley, except the resistive sierras area (these prisms were constrained). The 300 m slice (Figure 3b) shows a moderate resistivity of 100 ohm-m where the Colorado River passes through, meaning that body C represents the hydrological basin for the Colorado River. Starting with this depth slice, there appears to be a NNW trending feature that bounds the conductive western area (B) and the resistive eastern area (C). With this model we see that the hydrological basin deepens until 1000 m approximately.

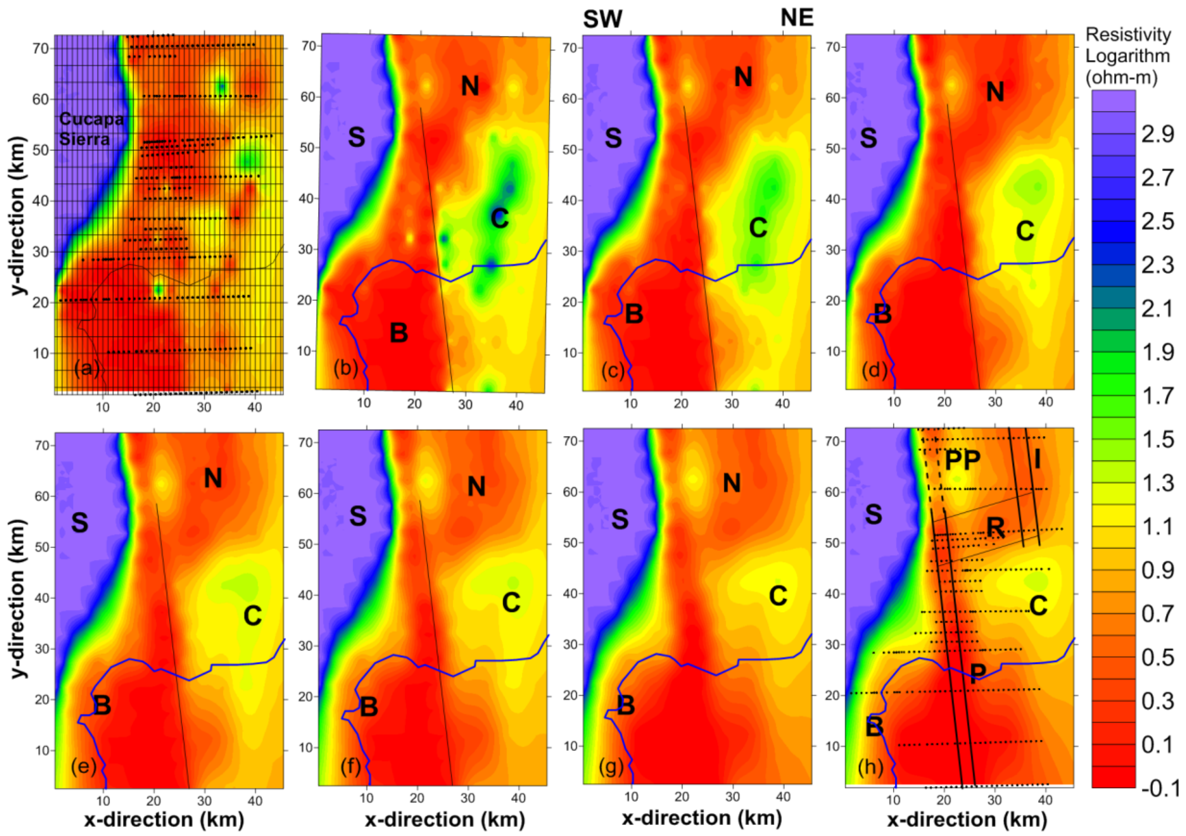

Figure 3: Three-dimensional resistivity model from the Cerro Prieto regional area. The model was sliced at: (a) 100 m depth, (b) 300 m, (c) 500 m, (d) 700 m, (e) 900 m, (f) 1150 m, (g) 1400 m, (h) 1800 m. In (a) is shown the horizontal dimensions of every prism. Dots indicate the SEV center locations. Capital letter means; S-sierra area, C-Colorado River resistive zone, B- south conductor, N-north conductor, P-Cerro Prieto alignment, PP-north continuation, I-Imperial alignment and R-rift conductor.

Figure 3e shows a conductive alignment between B and C. This is consistent with the Cerro Prieto fault location. Southward, there is surface evidence of this fault, but there are also seismic sections that detail the tectonics of this fault and others (Chanes-Martinez et al., 2013). However, there is no evidence of this fault northward. It has been traced by surface cracks when earthquakes occurred at this zone. These cracks are eroded in a very short time (Suarez-Vidal et al., 2007; 2008). The 1800 m deep slice in Figure 3h shows more alignments; the Cerro Prieto (P), the Imperial fault (I) alignments and a conductor between them (R) that can be the spreading center. The pair of faults and the spreading center form a pull-apart basin. Therefore a graben is formed at the R location. The local names for the north and south fault are the Morelia and Saltillo faults. Because of the prism discretization, we cannot say more about the inside of the spreading center. This R area is presently sinking because of the extensional forces or by the graben faults but also by the extraction of geothermal fluids. For the Imperial fault, there is geological evidence for this feature on the surface.

In the research area, there was no geophysical evidence of the on-land pull-apart basin before this study. The resistivity image in Figure 3h shows the trace of the San Andreas fault system and an on-land pull-apart basin. However, we can see a broad image. The faults have a 2.5 km horizontal thickness at a depth of 1800 m. We do not know why the faults are manifested as conductors.

A magnetotelluric resistivity section of the San Andreas fault close to Parkfield, California (Unsworth et al., 1999) shows the fault as a very good conductor. A similar study was done in Hollister, California (Bedrosian et al., 2004) showing the same behavior. In both papers they argue that serpentinites, clay and saline water could be the causes. But serpentinites and clay do not lower the rock resistivity so much. Therefore, saline fluids are the most probable. It is not clear where this saline water comes from. It could be the product of metamorphism in the fault zone.

REFERENCES

Aragon-Arreola, M., and Martin-Barajas, J.A.: Westward migration of extension in the northern Gulf of California, Mexico, *Geology*, **35**, (2007), 571-574.

Bedrosian, P.A., Unsworth, M.J., Egbert, G.D. and Thurber, C.H.: Geophysical images of the creeping segment of the San Andreas fault: implications for the role of crustal fluids in the earthquake process, *Tectonophysics*, **385**, (2004), 137-158.

Chanes-Martinez, J.J., Gonzalez-Escobar, M., Suarez-Vidal, F. and Gallardo-Mata, C.G.: Structural Geometry of a Sector of the Colorado River Delta, Baja California, Mexico, Based on Seismic Reflections, *Pure and Applied Geophysics*, (2013), DOI 10.1007/s00024-013-0729-z.

Charre-Meza, A.S.: Resistivity images obtained from collinear arrays from DC and application to Cerro Prieto Geothermal field, B.C., *M. S. Thesis*, (2000), CICESE.

Dorsey, R. and Martin-Barajas, J.A.: Sedimentation and deformation in a Pliocene–Pleistocene transtensional supradetachment basin, Laguna Salada, north-west Mexico, Basin Research, 11, (1999), 205-221.

Gill, P., Hammarling, S., Murray, W., Saunders, M., and Wright, M., 1986, Users's guide for LSSOL: A package for constrained linear least-squares and quadratic programming: Stanford Univ. Tech. Report SOL-886-1.

Perez-Flores, M.A., Mendez-Delgado, S. and Gomez-Treviño, E.: Imaging low-frequency and dc electromagnetic fields using a simple linear approximation, Geophysics, 66, (2001), 1067-1081.

Suarez-Vidal, F., Mendoza-Borunda, R., Nafarrete-Zamarripa, L.M., Ramirez, J. and Glowaka, E.: Shape and Dimensions of the Cerro Prieto Pull-Apart Basin, Mexicali, Baja California, Mexico, Based on the Regional Seismic Record and Surface Structures, *International Geology Review*, **50**, (2008), 636-649.

Suarez-Vidal, F., Munguia-Orozco, L. Gonzalez-Escobar, M., Gonzalez-Garcia, J. and Glowaka, E.: Surface Rupture of the Morelia Fault Near the Cerro Prieto Geothermal Field, Mexicali, Baja California, Mexico, during the Mw 5.4 Earthquake of 24 May 2006. *Seismological Research Letters*, **78**, (2007), 394-399.

Unsworth, M., Egbert, G. and Booker, J.: High-resolution electromagnetic imaging of the San Andreas fault in Central California, *Journal of Geophysical Research*, **104**, (1999), 1131-1150.

Wilt, M.J., Goldstein, N.E and Razo, M.A.: LBL resistivity studies at Cerro Prieto, *Second Symposium about the Cerro Prieto geothermal field*, (1978), LBL-7098, 179-188.

Wilt, M.J., Goldstein, N.E and Razo, M.A.: LBL resistivity studies at Cerro Prieto, *Third Symposium about the Cerro Prieto geothermal field*, (1979), LBL-94720, 419-428.